Laser Chem. 1983, Vol. 2, pp. 21–36
0278-6273/83/0206-0021$12.00/0

Printed in Great Britain

Laser Spectroscopy of Solids†

RICHARD G. BREWER and RALPH G. DeVOE

IBM Research Laboratory, San Jose, California 95193, USA

Remarkably narrow optical homogeneous linewidths of the order of 1 kHz have now been observed in low temperature zero-phonon transitions of dilute impurity ion crystals, such as Pr^{3+} in LaF_3. Novel nonlinear optical resonance techniques have been devised for this purpose using ultrastable phase locked cw dye lasers where the measurements are performed either in the frequency domain (hole burning) or in the time domain (coherent optical transients). These studies effectively bring the Mossbauer effect into the optical region. Hence, the observed linewidths are no longer limited by inhomogeneous strain broadening (~5 GHz) or even by static local fields due to neighboring spins (~100 kHz). However, weak magnetic field fluctuations from local spins are readily detected. As an example, spin decoupling and line narrowing, which are well known in NMR, are observed in an optical transition of Pr^{3+}:LaF_3 at 2 K where the ^{19}F–^{19}F dipolar interaction is quenched and the optical linewidth drops from 10 to 2 kHz, clearly demonstrating the spin broadening mechanism. Results will be discussed in terms of a Monte Carlo line broadening theory.

INTRODUCTION

Solids have long played an important role in the development of laser physics. Indeed, the first laser was a solid state device, namely, Maiman's ruby laser.[1] Shortly thereafter the field of nonlinear optics commenced when Franken *et al.*[2] transformed a ruby laser beam into its second harmonic by passing it through a quartz crystal. And the first coherent optical transient effect, the photon echo, was detected later in ruby by Hartmann *et al.*[3]

Laser spectroscopy,[4] on the other hand, has been concerned largely with atomic and molecular systems in the gas phase, and it is only recently that the new techniques of laser spectroscopy have been applied to solids. Within the last three years, for example, it has become clear that the optical homogeneous linewidths of certain rare

† This work is supported in part by the US Office of Naval Research.

earth impurity ion crystals can be exceedingly narrow, the order of 1 kilohertz or less.[5–7] These zero phonon transitions are the optical analogs of the Mossbauer effect. Such narrow linewidths suggest a number of new precision measurements, either in the time or frequency domain. In the time domain, coherent transients can be examined to reveal new aspects of the dynamic interactions occurring in solids. In the frequency domain, the structural details of solids can be probed as in nuclear magnetic resonance. Also, the possibility of developing solid state optical clocks exists and with it the potential for testing fundamental theories, such as the general theory of relativity.

In this article, I will restrict the discussion to recent dynamic studies of the optically active impurity ion Pr^{3+} in a host crystal of LaF_3 at $\sim$2 K. This study tests our understanding of the Pr^{3+} optical linebroadening and dephasing mechanisms, which are largely magnetic in origin, through such experimental optical techniques as free induction decay[5] and magic angle line narrowing.[6] This work has advanced recently to a new level of precision due to the development of a highly stable tunable ring dye laser that possesses a linewidth of about 300 Hertz.[8] On the theoretical side, our success with Monte Carlo calculations of linebroadening in Pr^3:LaF_3 will be reviewed.[9] Even more recently, we have been encouraged by an analytic treatment which explains the main features of linebroadening in this impurity ion solid and reveals as well limitations in the use of the optical Bloch equations for the case of solids.[10]

FREE INDUCTION DECAY THEORY

The two most important methods for measuring optical dephasing times have been the photon echo[3] and free induction decay (FID)[11] which we now consider. The simplest model is that of a collection of two-level atoms which are resonantly excited (prepared) by a coherent light wave. The atoms thereby are transformed from an initial stationary state to a superposition or mixed state which displays a time-dependent behavior both during the preparation stage and afterwards. Once the excitation is removed, the system freely radiates a coherent beam of light in the forward direction—the free induction decay effect. The atoms are perturbed of course by various time-dependent

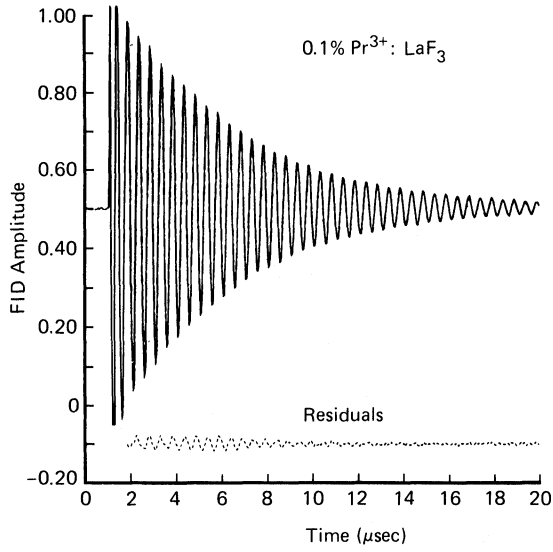

FIGURE 1 A computer plot of 400 points of optical FID of 0.1 at.% Pr^{3+}:LaF_3 at 1.6 K. The experimental data are overlayed on a damped cosine, and the residuals indicate that the dephasing time of 5.10 μs has an uncertainty of less than 1%. The signal is power broadened.

interactions which get them out of phase and produce a damped emission. An example of FID in Pr^{3+}:LaF_3 is shown in Figure 1.

BLOCH EQUATIONS

To interpret the observed decay rate, various theoretical models can be applied. We begin with the Schrödinger equation of motion in density matrix form

$$i\hbar\dot{\rho} = [H, \rho] + \text{relaxation terms} \tag{1}$$

which will be used to derive Bloch equation solutions[12] for a two-level atomic system before proceeding to more advanced cases. The Hamiltonian

$$H = H_0 + H_1$$

contains the free atom part H_0 with eigenenergies

$$E_i = \hbar\omega_i \qquad (i = 1, 2)$$

where $\omega_{21} = \omega_2 - \omega_1$ and the index 2 labels the upper state and 1 the lower state. In the presence of a light wave

$$E(z, t) = E_0 \cos(\Omega t - kz)$$

the atom undergoes a transition $1 \leftrightarrow 2$ due to the atom–field interaction

$$H_1 = -\mu \cdot E(z, t)$$

where the electric dipole matrix element is

$$\mu_{12} = \langle 1|\mu|2\rangle$$

The equations of motion for the slowly varying terms become

$$\dot{\tilde{\rho}}_{12} = (-1/T_2 + i\Delta)\tilde{\rho}_{12} + \tfrac{1}{2}i\chi(\rho_{22} - \rho_{11}) \tag{2a}$$

$$\dot{\rho}_{22} - \dot{\rho}_{11} = -(\rho_{22} - \rho_{11})/T_1 + (\rho_{22}^0 - \rho_{11}^0)/T_1 + i\chi(\tilde{\rho}_{12} - \tilde{\rho}_{21}) \tag{2b}$$

with the definition

$$\rho_{12} = \tilde{\rho}_{12}\, e^{i(\Omega t - kz)}$$

and neglecting nonresonant terms. Here, the Rabi frequency χ and the tuning parameter Δ are defined by

$$\chi = \mu_{12}E_0/\hbar \quad \text{and} \quad \Delta = -\Omega + \alpha + \omega_{21}$$

where α is a shift in the transition frequency ω_{21} due to an inhomogeneity in the local environment, i.e., static magnetic or crystalline Stark fields in the case of Pr^{3+}:LaF_3.

In the optical Block model, the decay behavior is introduced in (2) by phenomenological population and dipole times T_1 and T_2 as in NMR. Thus, with the definitions

$$u = \tilde{\rho}_{12} + \tilde{\rho}_{21} \qquad v = i(\tilde{\rho}_{21} - \tilde{\rho}_{12}) \quad \text{and} \quad w = \rho_{22} - \rho_{11}$$

we cast (2) into the Bloch equation[13]

$$\frac{dB}{dt} = \beta \times B$$

which describes a precessional motion of the Bloch vector B about

an effective field β with components

$$B = iu + jv + kw$$

$$\beta = i\chi + k\Delta$$

This is mathematically equivalent to a spin precessing in a magnetic field.[14]

Bloch equation solutions are derived from (2) using a Laplace transform technique[15] and yield for the steady-state preparation

$$\tilde{\rho}_{12}(0) = \frac{i\chi(-i\Delta + 1/T_2)(\rho_{22}^0 - \rho_{11}^0)/2}{\Delta^2 + 1/T_2^2 + \chi^2 T_1/T_2} \tag{3}$$

At time $t = 0$, the excitation ends and the FID begins because the laser frequency is switched suddenly to a new value ($\Omega \to \Omega'$). The FID solution follows from (2a) as

$$\tilde{\rho}_{12}(t) = \tilde{\rho}_{12}(0)\, e^{(-1/T_2 + i\Delta)t} \qquad t > 0 \tag{4}$$

The FID expressed as a field amplitude

$$E_{12}(z, t) = \tilde{E}_{12}(z, t)\, e^{i(\Omega t - kz)} + \text{c.c.}$$

obeys Maxwell's wave equation

$$\frac{\partial \tilde{E}_{12}}{\partial z} = -2\pi i k N \mu_{12} \langle \tilde{\rho}_{12}(t) \rangle \tag{5}$$

where the bracket

$$\langle \tilde{\rho}_{12}(t) \rangle = \frac{1}{\sqrt{\pi}\sigma} \int_{-\infty}^{\infty} g(\Delta) \rho_{12}(\Delta, t)\, d\Delta \tag{6}$$

denotes an average over a Gaussian inhomogeneous lineshape $g(\Delta) = e^{-(\Delta/\sigma)^2}$. The observed FID signal appears as a heterodyne beat

$$F(t) = \tfrac{1}{2} E_0 \tilde{E}_{12}\, e^{i(\Omega - \Omega')t} + \text{c.c.} \tag{7}$$

due to the laser frequency switch $\Omega \to \Omega'$ at $t = 0$, a process which terminates the excitation of the initially prepared packet and allows sensitive detection of the free precession signal with low noise. Omitting trivial factors, the resulting FID Bloch solution is of the form

$$F(t) \sim \chi^2 \left[1 - \frac{1}{\sqrt{1 + \chi^2 T_1 T_2}}\right] e^{-(t/T_2)(1 + \sqrt{1 + \chi^2 T_1 T_2})} \cos(\Omega - \Omega')t \tag{8}$$

The preexponential factor displays a nonlinear intensity dependence in contrast to NMR where FID is a first order process due to the small inhomogeneous broadening. Similarly, the damping term in (8) exhibits power broadening through the term $\chi^2 T_1 T_2$ where $T_1 \gg T_2$ in Pr^{3+}:LaF_3. In the limit $\chi^2 T_1 T_2 \ll 1$, the decay time becomes $\frac{1}{2}T_2$.

While the Bloch theory has played an important role in NMR and quantum optics, it also is limited in that it ignores the details of the basic dipolar interactions such as Pr^{3+}–F and F–F which broaden the Pr^{3+} optical transition. It also ignores the presence of a frozen core of fluorine nuclei surrounding each Pr^{3+} ion, the LaF_3 crystal structure, and the dependence of linewidth on the Pr^{3+} ($I = 5/2$) magnetic substate. Before considering the Monte Carlo calculation which overcomes these difficulties, let us consider the current status of the experiments.

FREE INDUCTION DECAY EXPERIMENTS

The optical Pr^{3+} transition of interest is $^3H_4 \rightarrow {}^1D_2$ which lies conveniently in the yellow region at 5925 Å. Due to the low electric field site symmetry (C_2), all electronic degeneracy is removed. Thus, for the ground electronic state $^3H_4$, there are $2J + 1 = 9$ Stark split *singlet* states with splittings of order 50 cm^{-1}. Consequently, as noted by Bleaney[16] and by Teplov,[17] all first order magnetic hyperfine interactions vanish in the absence of an external magnetic field. The nuclear quadrupole interaction and the second order magnetic dipole hyperfine interaction generate three doubly degenerate hyperfine states for each Stark split singlet ($I_Z = \pm 5/2$, $\pm 3/2$ and $\pm 1/2$ since $I = 5/2$) with splittings of the order of 10 MHz. Only the lowest crystal field Stark split states of $^3H_4 \rightarrow {}^1D_2$, the zero phonon line, are examined. Hence, three equally intense optical transitions occur, $I''_z \leftrightarrow I'_z = \pm 5/2 \leftrightarrow \pm 5/2$, $\pm 3/2 \leftrightarrow \pm 3/2$, and $\pm 1/2 \leftrightarrow \pm 1/2$, and overlap because of the large inhomogeneous strain broadening of ~5 GHz.

The technique for observing optical FID relies on laser frequency switching[18] as shown in Figure 2.[5] The external beam of a phase-locked cw ring dye laser of high frequency stability passes through an acousto-optic modulator prior to exciting a 0.1 at.% Pr^{3+}:LaF_3 crystal which is immersed in liquid helium at ~1.6 K. A single packet

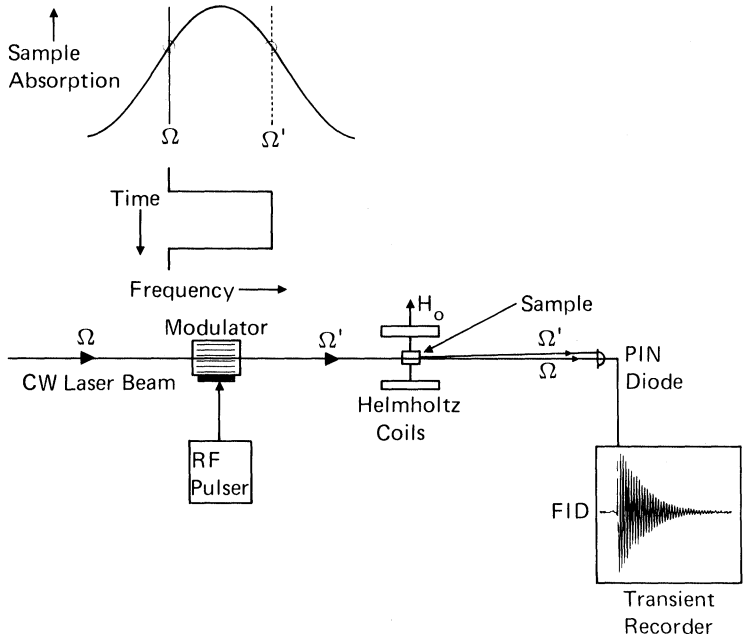

FIGURE 2 Acousto-optic modulator laser frequency switching technique for observing coherent optical transients such as FID and photon echoes.

of Pr^{3+} ions within the inhomogeneous lineshape is coherently prepared by a laser beam (~5 mW at the crystal) when the modulator is driven by a 110 MHz r.f. source which is gated on for a 400 μs period. FID follows when the rf frequency is switched suddenly from 110 to 105 MHz and is detected by a photodiode as a 5 MHz heterodyne beat signal in transmission.

LASER PHASE LOCKING

To detect ultraslow dephasing times by FID, the laser frequency must remain fixed within the Pr^{3+} homogeneous linewidth for the preparation interval $\sim T_2$, otherwise the observed decay merely reflects laser frequency jitter. Figure 3 shows a phase modulation technique for phase/frequency locking a ring dye laser to a reference cavity. The

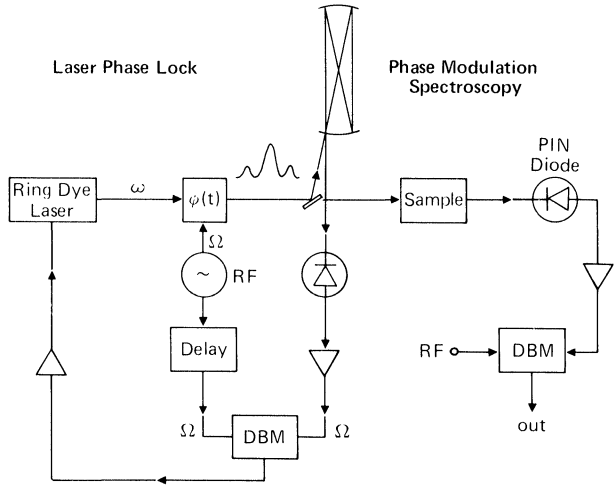

FIGURE 3 Schematic of apparatus for phase-locking a cw ring dye laser. The sample and detection circuit to the right show how narrow hole burning signals can be detected by phase modulation spectroscopy with basically the same apparatus.

method, which was proposed by Drever, has yielded laser linewidths as narrow as ~100 Hertz.[19,8] A part of the external beam of the laser is phase modulated by passing it through an electro-optic crystal that is driven continuously by a 40 MHz r.f. generator, and the beam then strikes an acoustically isolated 50 cm confocal reference cavity having a 1.5 MHz bandwidth. The laser field now contains pairs of sidebands located symmetrically about the center frequency. When the center frequency coincides with a mode of the reference cavity, the central component will be stored in the cavity for its ringing time while the sidebands will be reflected at the end mirror. For this condition, the reflected light and some of the stored light which leaks out of the cavity will produce at a photodiode two heterodyne beats of opposite phase which just cancel. If, however, the laser phase or frequency fluctuates, this balanced condition will be upset because the stored light retains memory of the laser's frequency at a previous instant while the reflected light monitors the instantaneous laser frequency. In this circumstance, the two heterodyne beat signals no longer cancel but produce an error signal in a fast high gain servo loop that drives the laser frequency to a stable operating point.

Important advantages of this method are (1) Laser amplitude noise can be reduced to the shot noise limit because the beat frequency can be selected in a region where the laser noise is low and because the balancing technique automatically eliminates laser noise not associated with the error signal. (2) The response time of the optical cavity is fast in the reflection mode allowing a large servo loop bandwidth and thus a narrow laser linewidth. (3) The heterodyne beat error signal can be monitored in a dispersion mode (Figure 4) which offers a sharp discriminant and locates the lock point at zero amplitude, independent of the size of the error signal. In Figure 4, the phase-locked laser beam is monitored with a second 50 cm confocal cavity and shows that the laser linewidth is no larger than 300 Hertz rms.

The phase modulation technique can be used also for detecting low amplitude noise lineshapes (hole-burning) under steady-state conditions as demonstrated initially by Bjorklund.[20,21] In combination with a laser of high frequency stability, extraordinarily high resolution optical studies can now be performed in solids.

DATA ACQUISITION

The realization of tunable lasers of high frequency stability, assures that FID or other coherent transients with long optical dephasing times can be monitored reproducibly with high precision. Figure 1 shows the excellent fit of a damped cosine function which is overlayed on 400 experimental points of the Pr^{3+}:LaF_3 data. In fact, the two curves cannot be distinguished and the residuals indicate that the decay time can be determined to an uncertainty of less than 1%. The experimental points were acquired from an analog signal using a transient digitizer, and the data was stored in an IBM Personal Computer and then transferred to an IBM 3033 computer for least squares analysis, graphics or other data handling.

MAGIC ANGLE LINE NARROWING

The FID technique offers a way of measuring the optical homogeneous linewidths of a solid such as Pr^{3+}:LaF_3 without the influence of

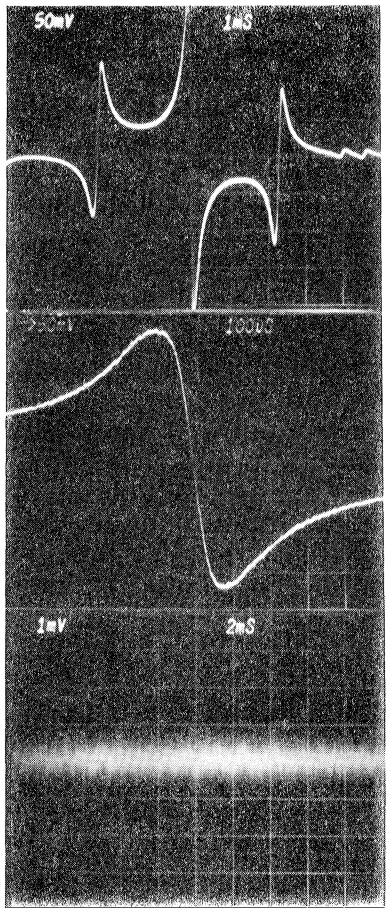

FIGURE 4 Top two traces: Experimental dispersive lineshape of a phase-locked laser beam (40 MHz modulation frequency) as seen by a frequency swept 50 cm confocal cavity in reflection. The laser beam is phase locked to a second 50 cm cavity and exhibits in the third trace, where the first cavity is not swept, a 300 Hz rms laser linewidth.

inhomogeneous broadening. Thus, in Figure 1 the linewidth is about 10 kHz HWHM, i.e., about the same magnitude as that encountered in NMR. What is the broadening mechanism? The $^1D_2$ radiative lifetime of 0.5 ms sets a limiting value of 160 Hertz HWHM; phonon-ion interactions at 1.6 K are negligible at this point in time as are

Pr^{3+}–Pr^{3+} interactions in the dilute samples studied. The dominant effect is the fluctuating part of the Pr–F magnetic dipolar interaction.

The dipolar mechanism has been demonstrated convincingly by an optical magic angle line narrowing experiment[6] which we now discuss. The pulse sequence is shown in Figure 5 and involves not only laser frequency switching for producing FID but the simultaneous application of an rf pulse in near resonance with ^{19}F nuclei. The basic idea is that pairs of F nuclei throughout the crystal undergo mutual spin flips which produce a fluctuating magnetic field at each Pr^{3+} site. The $^1D_2$ and $^3H_4$ states of Pr^{3+} fluctuate in energy correspondingly and thus the optical transition broadens. With a suitable r.f. field applied, the F precessional motion about its effective field tends to average out the F–F dipolar interaction and as a result the Pr–F dipolar interaction is quenched (see Figure 6). This effect can be viewed as a kind of motional narrowing. A detailed theory, which is given elsewhere,[6] predicts that the Pr^{3+} linewidth is given by

$$\Delta\nu(\beta) = \Delta\nu(0)\cos\beta \cdot \tfrac{1}{2}(3\cos^2\beta - 1) \tag{9}$$

where $\beta = \tan^{-1}(\gamma_F B_x/\Delta_F)$ is the angle that the effective field of the F nucleus makes with the z axis in its rotating frame, B_x being the r.f. field amplitude. From (9), we see that the Pr^{3+} linewidth should drop to zero when $\beta = \pi/2$, the F resonance condition, and $\beta = \cos^{-1}(\sqrt{3}/3)$, the magic angle condition. In practice, the linewidth drops from 10 to 2 kHz, but the measurements should be repeated using the improved phase locked laser to determine the origin of the

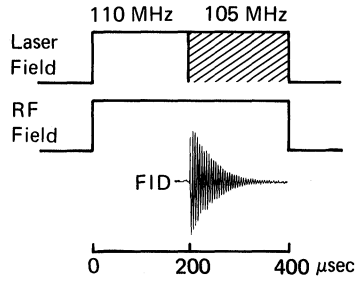

FIGURE 5 Magic angle pulse sequence showing the laser field frequency shift and the F spin decoupling radio frequency field with time. The Pr^{3+} ions are coherently prepared by the laser field in the initial 200 μs interval and then exhibit optical FID when the laser frequency is suddenly switched 5 MHz at $t = 200$ μs.

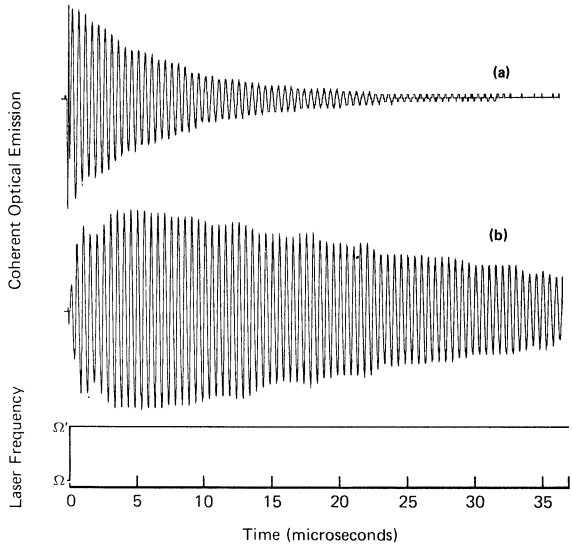

FIGURE 6 Optical FID in 0.1% Pr^{3+}:LaF_3 at 1.8 K in the presence of a static magnetic field $B_0 = 130\ \text{G} \pm c$ axis: (a) with no r.f. field where $T_2 = 15.6\ \mu\text{s}$ (10.2 kHz) and (b) under magic angle conditions with an r.f. field $B_x = 25\ \text{G}$ where $T_2 = 66\ \mu\text{s}$ (2.4 kHz).

residual width. Figure 7 shows that the experimental results agree rather well with Eq. (9) and thus unequivocally verifies the magnetic dipolar broadening mechanism.

MONTE CARLO THEORY[9]

We now require a more detailed theory of linebroadening than the simplistic T_1, T_2 description of the Bloch equations. We first replace Eq. (2a) by

$$\dot{\rho}_{12} = (-\gamma + i(\Delta + \delta\omega(t))\tilde{\rho}_{12} + \tfrac{1}{2}i\chi(\rho_{22} - \rho_{11}) \tag{10}$$

where the Pr^{3+} transition frequency fluctuates as

$$\delta\omega(t) = -(\gamma_I' - \gamma_I'')\gamma_s\hbar \sum_k \frac{3\cos^2\theta_k - 1}{r_k^3} I_k S_{kz}(t) \tag{11}$$

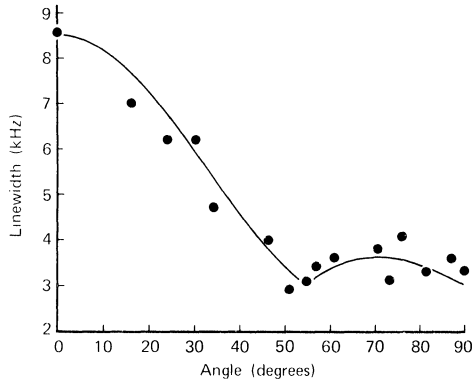

FIGURE 7. Pr^{3+} optical linewidth versus angle β expressed in degrees. Solid circles: experimental points for the case $B_0 = 130G \| c$ axis and $B_x = 25$ G. Solid curve: Eq. (9) with frequency offset of 3 kHz included for residual broadening.

due to random flipping of the fluorine spin $S_z(t)$ arising from F—F mutual spin flips which affect the secular part of the Pr—F dipolar interaction. Here, the F spin is labeled S and the Pr spin I, the population decay term $\gamma = \frac{1}{2}(\gamma_1 + \gamma_2)$, and the gyromagnetic ratio of the $^1D_2$ and $^3H_4$ states are γ_I' and γ_I''. The FID solution of (10) now assumes the form

$$\langle \tilde{\rho}_{12}(t) \rangle = \left\langle \tilde{\rho}_{12}(0) \exp\left[(-\gamma + i\Delta)t + i \int_0^t \delta\omega(t')\, dt' \right] \right\rangle \qquad (12)$$

The quantity $\tilde{\rho}_{12}(t)$ involves the phase history of a single Pr^{3+} ion and therefore must be averaged over the distribution of frequency fluctuations occurring at different Pr^{3+} sites both during the preparative period $t \leqslant 0$ and afterward $t \geqslant 0$. In addition, averages are to be performed over the local inhomogeneous static magnetic and crystalline Stark fields.

The following assumptions enter into the calculation. (1) The sudden jump approximation of the kth fluorine spin $S_{kz}(t)$ assumes that it can have only two values $+1/2$ and $-1/2$ and that it jumps instantaneously between these two values at random times and positions in the lattice at an average rate W. (2) The LaF_3 crystal structure ($P3Cl$–D_{3d}^3) is assumed for the nearest 125 unit cells (2250 fluorines) surrounding a Pr site. (3) The c axis of the LaF_3 crystal is parallel to

an external magnetic field. (4) The number of fluorine spin flips per unit time follows a Poisson distribution.

The resulting computer program is not only capable of generating the Pr^{3+} optical homogeneous linewidth but the static magnetic inhomogeneous linewidth as well. Table I summarizes these calculations and the current experimental results. For an r.f. transition of the $^3H_4$ Pr^{3+} ground state, a value of 82 kHz is obtained for the inhomogeneous magnetic broadening which compares favorably to a Van Vleck second moment calculation and to optically detected rf measurements for external fields in excess of the local field of 16 G.

Notice in Figure 8 that the optical dephasing time is rather insensitive to the assumed fluorine mean flip time T. Actually, the parameter T need not be assumed, but rather it can be calculated from the method of moments[24] to be $T \sim 10T_2 = 170$ μs which yields a 19 μs (16.8 kHz) dephasing time compared to the experimental value 15.8 μs (20.1 kHz). The agreement is unusually good by the standards of previous theories considering that the discrepancy is only 15%.

Other conclusions emerge from these studies largely due to the fact that only a few fluorine nuclei, those close to the Pr^{3+} site, are found to contribute to optical dephasing. For example, our lattice size of 2250 fluorine is about two orders of magnitude larger than necessary. Secondly, the small number of fluorines required implies that correlations between nearby fluorines do not strongly affect the

TABLE I
Linewidths of ^{141}Pr in LaF_3 due to magnetic broadening

Transition	Method	Linewidth FWHM (kHz)
		Inhomogeneous
r.f. ($\Delta I_z'' = \pm 1$)	Monte Carlo theory	82
	Van Vleck second moment	84.5
	cw rf-optical double resonance[22]	
	$I_z'' = 1/2 \rightarrow 3/2$	180 ± 10^a $(\sim 100)^b$
	$I_z'' = 3/2 \rightarrow 5/2$	200 ± 10^a $(\sim 100)^b$
	Optically detected r.f. transients[23]	
	$I_z'' = 3/2 \rightarrow 5/2$	230 ± 25^a
		Homogeneous
Optical ($^3H_4 \leftrightarrow {}^1D_2$)	Monte Carlo theory	16.8
($\Delta I_z = 0$)	FID experiment[5]	20.2^b

[a] Earth's magnetic field.
[b] Static external field ≥16 G.

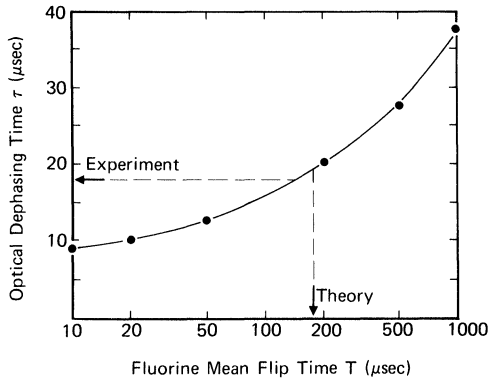

FIGURE 8 The Pr^{3+} optical dephasing time versus the fluorine mean flip time T. The optical FID result is 15.8 μs and the theoretical fluorine spin flip time $T = 170$ μs.

optical linewidth. Thirdly, the static Pr^{3+} magnetic moment can polarize the nearest neighbor fluorines and detune them from the bulk fluorines so that they are incapable of undergoing spin flips. This frozen core effect, which is well known in ESR, reduces the Pr^{3+} linewidth from the value it would have if the nearest neighbors were also flipping. Inclusion of the frozen core model in the Monte Carlo calculation shows, contrary to intuition, that the optical linewidth varies slowly with the Pr^{3+} magnetic moment $\mu_z^{Pr} = \gamma_I I_z \hbar$ or magnetic substate I_a.

GAUSSIAN MODULATION MODEL

Very recently, we have attempted to obtain analytic solutions for the optical dephasing problem using a Gaussian modulation model. This approach, which will be reported elsewhere,[10] has enjoyed some success and should be a useful method in the future for describing the nature of optical dephasing in these many body systems.

References

1. T. H. Maiman, *Nature* **187,** 493 (1960).
2. P. A. Franken, A. E. Hill, C. W. Peters and G. Weinrich, *Phys. Rev. Lett.* **7,** 118 (1961).
3. N. A. Kurnit, I. D. Abella and S. R. Hartmann, *Phys. Rev. Lett.* **13,** 567 (1964).

4. See for example *Laser Spectroscopy V*, ed. A. R. W. McKeller, T. Oka and B. P. Stoicheff (Springer-Verlag, New York, 1981).
5. R. G. DeVoe, A. Szabo, S. C. Rand and R. G. Brewer, *Phys. Rev. Lett.* **42,** 1560 (1979).
6. S. C. Rand, A. Wokaun, R. G. DeVoe and R. G. Brewer, *Phys. Rev. Lett.* **43,** 1868 (1979).
7. R. M. Macfarlane, R. M. Shelby and R. L. Shoemaker, *Phys. Rev. Lett.* **43,** 1726 (1979).
8. R. G. DeVoe and R. G. Brewer (unpublished).
9. R. G. DeVoe, A. Wokaun, S. C. Rand and R. G. Brewer, *Phys. Rev. B* **23,** 3125 (1981).
10. E. Hanamura, R. G. DeVoe and R. G. Brewer (to be published).
11. R. G. Brewer and R. L. Shoemaker, *Phys. Rev. A* **6,** 2001 (1972).
12. R. G. Brewer, in: *Frontiers in Laser Spectroscopy*, Les Houches Lectures (North-Holland, New York, 1977) p. 341.
13. F. Block, *Phys. Rev.* **70,** 460 (1946).
14. R. P. Feynman, F. L. Vernon and R. W. Hellwarth, *J. Appl. Phys.* **28,** 49 (1957).
15. A. Schenzle and R. G. Brewer, *Phys. Rev. A* **14,** 1756 (1976).
16. B. Bleaney, *Physica (Utrecht)* **69,** 317 (1973).
17. M. A. Teplov, *Zh. Eksp. Teor. Fiz.* **53,** 1510 (1967) [*Sov. Phys. JETP* **26,** 872 (1968)].
18. A. Z. Genack and R. G. Brewer, *Phys. Rev. A* **17,** 1463 (1978); R. G. Brewer and A. Z. Genack, *Phys. Rev. Lett.* **36,** 959 (1976).
19. R. W. P. Drever, J. L. Hall, F. V. Kowalski, J. Haugh, G. M. Ford and A. Munley (unpublished).
20. G. C. Bjorklund, Opt. Lett. **5,** 15 (1980); G. C. Bjorklund and M. D. Levenson, *Phys. Rev. A* **24,** 166 (1981).
21. The theory of phase modulation laser spectroscopy is described in A. Schenzle, R. G. DeVoe and R. G. Brewer, *Phys. Rev. A* **25,** 2606 (1982).
22. L. E. Erickson, *Phys. Rev. B* **16,** 4731 (1977).
23. R. M. Shelby, C. S. Yannoni and R. M. Macfarlane, *Phys. Rev. Lett.* **41,** 1739 (1978).
24. N. Bloembergen, *Physica (Utrecht)* **15,** 386 (1949); I. J. Lowe and S. Gade, *Phys. Rev.* **156,** 817 (1967).